Popigai and Chicxulub craters: multiple impacts and their associated grabens

Jaroslav Klokočník[1], Václav Cílek[2], Jan Kostelecký[3,4], Aleš Bezděk[1]

[1]Astronomical Institute, Czech Academy of Sciences, CZ 251 65 Ondřejov, Fričova 298, Czech Republic, jklokocn@asu.cas.cz; bezdek@asu.cas.cz
[2]Geological Institute, Czech Academy of Sciences, Prague, CZ 165 00 Praha 6, Rozvojová 269, Czech Republic, cilek@gli.cas.cz
[3]Research Institute of Geodesy, Topography and Cartography, CZ 250 66 Zdiby 98, Czech Republic
[4]Faculty of Mining and Geology, VSB-TU Ostrava, CZ 708 33 Ostrava, Czech Republic, kost@fsv.cvut.cz

Correspondence to: Jaroslav Klokočník (jklokocn@asu.cas.cz)

Abstract. More advanced data (gravity field model EIGEN 6C4 including the GOCE gradiometry data instead of EGM2008) and a more sophisticated method (using a set of the gravity aspects instead of the gravity anomalies and the radial second derivative of the disturbing potential only) enable a deeper study of various geological features. The improved techniques were applied to study the impact craters Chicxulub and Popigai. We confirm our results from 2010, extend them, and offer more complicated models, namely by means of the gravity strike angles. Both craters are interpreted to be double or multiple craters. The probable impactor azimuth was from NE (to SW) for Chicxulub and SE (to NW) for Popigai. Formation of both the craters seem to be associated with impact induced tectonics that triggered development of impact grabens.

1. Motivation

In 2010, we published (Klokočník et al., 2010, in this journal) results of our tentative analysis of the gravity data for two areas of proven, huge impact craters Chicxulub and Popigai. The analyses were based on the global combined gravity model EGM 2008 (Pavlis et al. 2008 a,b, 2012) to degree and order (d/o) = 2159, top of the modelling of the gravity field of the Earth at that time as for precision and resolution. We suggested (in Klokočník et al., 2010) that Chicxulub (north Yucatán, México) may be a double crater and Popigai (north Siberia, Russia) may be a multiple crater [see the labels "Popigai I-IV", according to Rajmond's catalogue (2009), on © Google Earth]. The craters II-IV are not yet proven impact crater candidates. Altogether they would create a hypothetical Popigai crater's family, a catena (see Supplement S3). We analyzed gravity anomalies and second radial components of the Marussi tensor. Now, we work with a set of the gravity aspects (incorporating those two functions, too).

Since that time we have analysed many geological features on the Earth, the Moon and Mars, we make use of new gravity models and other data sources (see below) and we summarized our results in three books and about 15 papers (e.g., Klokočník & Kostelecký 2015, Klokočník et al., 2017, 2018, 2020, 2021, 2022 a,b, 2023 a,b).

We (and the readers) are well aware that solely the gravity data are not unambiguous to detect ground density anomalies (causative bodies); we always need and seek for additional data (geological, geophysical, seismic, topography, archaeology). Therefore, with our data and method, we offer only a step to possible field explorations and subsequent interpretations but not a confirmation of the structures.

With increasing precision, accuracy, resolution and reliability of our knowledge about the gravity and magnetic fields, we can test diverse applications impossible before. This is not only about data available, it is also about methodology; the traditional gravity anomalies are no longer sufficient. We apply a set of the *gravity aspects* instead (Sect. 2 and Supplement S1).

Another impetus for this study was a similarity of the two craters in the sense that they are directly associated with close linear structures that seemingly have nothing to do with the impact event, but occur closely to the craters. This could be a coincidence of two different, genetically independent geological phenomena, or a sign of existence of a trench being modified by the impact event. The impact shock affects the entire region and those previously existing faults or fault zones that were in an extensional tectonic regime were activated to form an impact graben**.**

This paper is a revival concerning our previous findings about *Popigai* and *Chicxulub*. Now we have (in comparison with Klokočník et al., 2010) better tools (the set of the gravity aspects) and a better gravity model (EIGEN6C4, with GOCE data), thus we can support or reject those older results. We offer new and hopefully more convincing results in favour of a double/multiple character of both Chicxulub and Popigai craters. These results are not in conflict nor with known geology of the areas nor with the information from magnetic intensities (not studied here, see, e.g. Hildebrand et al., 1998, Urrutia-Fucugauchi et al., 2022, or Mendes et al., 2023).

Many figures which may help the reader are gathered in *Supplementary materials* in S*i*: there is S2 tutorial, with tests about artefacts, S3 for Popigai, and S4 for Chicxulub. The theory is shortly repeated in S1. Link: https://www.asu.cas.cz/~jklokocn//CHIC-POP24_supplements/.

2. Notes on theoretical preliminaries

Gravity (gravitational) aspect (descriptor) is a functional/function of the disturbing gravitational field potential T_{ij}. We work with the gravity anomaly (or disturbance) Δg, the Marussi tensor ($\mathbf{\Gamma}$) of the second derivatives of the disturbing potential (T_{ij}), two gravity invariants (I_j), their specific ratio (I), the strike angles (θ) and the virtual deformations (*vd*).

The theory came mainly from Pedersen & Rasmussen (1990) and Beiki & Pedersen (2010). The theory with examples is summarized in our books (Klokočník et al., 2017, 2020, 2022b); it cannot be (due to space reasons) repeated here (see Supplement S1). Only a few notes follow.

The gravity aspects are sensitive in various ways to the underground density contrasts (variations) due to the causative bodies, exciting the relevant gravity signals. The set of the gravity aspects tells us much more about the causative body than the traditional Δg only. It informs about the location, shape, orientation, a tendency of the ground structure to 2D or 3D patterns, stress trends and may simulate a "dynamic information" about existing tensions (although the input data are always the harmonic geopotential coefficients of a *static* gravity model).

For example, the strike angle θ mathematically can be the main direction of the Marussi tensor $\mathbf{\Gamma}$ of the second derivatives of the disturbing potential (the first column and first row of $\mathbf{\Gamma}$ is identically equal zero for this preferred direction). The strike angle is, from the geophysical point of view, a direction important for description of the ground structures. It may indicate areas with a lower density or higher porosity or a "stress direction" or both or the areas under a strong influence of rapid and/or intensive geomorphic processes. When I=0, the values of θ may be symptomatic of a flat causative body. For more details see Beiki & Pedersen (2010) and our S1.

A usual situation is that the strike angle θ has diverse directions, as projected on the Earth' surface. The *combed strike angles* are the strike angles oriented roughly in one and the same direction in the given area. Theory for the "combed" strike was explained, together with relevant statistics, in Klokočník et al. (2019). For statistical use we defined a degree of alignment of the strike angles by the "comb coefficient" (*Comb*) as a relative value in the interval $\langle 0,1 \rangle$. Zero *0* means that the strike angles are „not combed" (totally dishevelled, the vectors θ are in diverse directions); *1* means "perfectly combed" (perfectly kempt, the vectors of θ are oriented into one prevailing direction). If *Comb* is smaller than 0.55, we say that θ_i of the given region are "not combed"; if *Comb*>0.65, we say that θ_i are "combed", and for *Comb*>0.99, they are perfectly

aligned. The alignment may take a linear form (e.g. along a fault) or can take the shape of a halo (around craters); see *Theory* in S1 and many examples in the tutorial supplement S2.

Link: *https://www.asu.cas.cz/~jklokocn//CHIC-POP24_supplements/.*

3. Data, computation, and figures

We always start all our computations with the harmonic geopotential coefficients (Stokes parameters) of the static global gravity field models as the input data; they describe the gravitational potential of the Earth. The whole theory is prepared in such a way that we cannot use another input than the harmonic coefficients (Pedersen & Rasmussen, 1990; Beiki & Pedersen, 2010; Klokočník et al. 2017, 2020, 2022b).

We make use of a high resolution combined *E*uropean *I*mproved *G*ravity model of the *E*arth by *N*ew techniques (*EIGEN 6C4*, Förste et al., 2014), expanded to degree and order (d/o) 2190 in spherical harmonics; this corresponds to the ground resolution 5x5 arcmin or ~9 km on surface. Precision of EIGEN 6C4, expressed in terms of Δg, is N=10 mGal, but in many civilized land areas and over the oceans and open seas is much better. The authors of EIGEN 6C4 did not have access to most of the recent high resolution terrestrial gravity data on the continents, thus they took a synthesized gravity anomaly grid based on EGM2008 (Pavlis et al., 2008 a,b, 2012). That means that the errors for high d/o terms in EIGEN 6C4 are dominated by the relevant errors in EGM2008. To estimate the actual, realistic precision for the given area of interest – not only for a general figure 10 mGal – one needs to inspect gravity anomaly commission error maps of EGM2008 (Pavlis et al. 2008 a,b; also in S3). It was accounting a complete covariance matrix between the solved-for harmonic coefficients in this gravity model. Using those maps for the northern Yucatan peninsula, we get N=4-8 mGal. For Popigai in Siberia, it is ~15 mGal.

Note about other data sources: *ETOPO 1* global surface topography (Amante and Eakins, 2009), a global 1' relief model of the Earth surface that integrates land topography and ocean bathymetry from a large number of satellite and other measurements. Its precision globally should be 10 m in heights, its accuracy ~30 m.

There are alternative topography data files (not fully independent of the Etopo files), like various versions of ASTER GDEM (JPL NASA and Japan), SRTM (NASA), GEBCO, and ETOPO 2022 release. Google Earth is also helpful.

Bedmap 2 is a subglacial topography valid for Antarctica (Fretwell et al., 2013). It contains the bedrock elevation beneath the grounded ice sheet. It is given as a 1x1 km grid of height of the bedrock above sea level, but actual measurements are often much sparser. We also worked with the *RET 14* (Hirt et al., 2016), a degree-2190 gravity field model *SatGravRET2014*, given as a set of harmonic geopotential coefficients, meaningful only for the continent of Antarctica (not globally!). Roughly speaking, it combines the global gravity field model *EIGEN 6C4* and the Bedmap 2 topography.

The data for magnetic analysis on the Earth are the grid value from the worldwide EMAG 2 model for magnetic intensities (Maus et al., 2009). There are also gravity filed models, global topography, and magnetic data for the Moon and Mars; gravity field models of the Moon and Mars provide already sufficient ground resolution for our analysis. It is about 10 km for the Earth and the Moon, but only 130 km for Mars. We present examples based on these gravity models in S2.

We computed the gravity aspects over many regions of the world in a step 5x5 arcmin in latitude and longitude, corresponding to the ground resolution of 9 km. But we can also use (and use here) a 4 km resolution without any degradation of the results (we offer some results of our truncation error tests and testing of artefacts in Klokočník et al., 2021 and here in Sect. 4 and S2). This higher resolution sometimes adds a new and valuable information.

The numerical stability of computations of high degree and order functions in the aspects is extremely important; it was intensively investigated, tested and is guaranteed to much higher degree and order than we need here (work done during last about ten years by the co-authors of this paper, plus Sebera et al. 2013 and Bucha & Janák, 2013).

Our figures are not generated by an automat, but created manually and individually with specific scales to emphasize various features and details. We plot all the quantities in geodetic (geographic) latitudes and East longitudes.

The gravity disturbances (anomalies) are given in milliGals [*mGal*], the second order derivatives are in Eötvös [*E*]. Let us recall that $1mGal = 10^{-5}\, ms^{-2}$, $1E \equiv 1$ Eötvös $= 10^{-9}\, s^{-2}$. The invariants have units I_1 [s^{-4}] and I_2 [s^{-6}]. The strike angle θ [^{o}, *deg*] is expressed in degrees with respect to the local meridian; its red colour means its direction to the east and blue to the west of the meridian. Often, we plot θ black and white only. The strikes are shown in a regular grid 5x5 arcmin; it has not any geophysical meaning, this is just the choice for plotting.

4. Artefacts

4.1.Our previous work

To avoid various mis-interpretations we need to test the input data to our analyses in various ways (e.g., Klokočník et al., 2021). We made our best to avoid the artefacts, but nevertheless, they cannot be excluded (S4: slides # >23). The important facts are the resolution and statistical significance.

The *ground resolution* (GR) of the gravity field model is derived from maximum d/o of its spherical harmonic expansion (the definition of GR is in S2: 23), more in Sect 4.2.

Another important factor is the signal-to-noise ratio $R=S/N$. The "signal" S is given as the range of gravity anomalies in the area of interest. The noise N is the commission error of the gravity anomalies Δg (see figure in S1, last page) or the estimated precision of Δg of EIGEN 6C4. We need $R > 3$ to have statistically significant results. We have:

$$\min R = (\min (\max|-S|, \max + S))/(\max N);$$
$$\max R = (\max (\max|-S|, \max + S))/(\min N).$$

With the figure from S1, defining N, figures below and in S3 and S4, defining S, for Δg of Popigai and Chicxulub, we get $R_{(\min,\max)} = 8–15$ for Popigai and $R_{(\min,\max)} = 5–20$ for Chicxulub.

4.2. Resolution

The reader certainly knows about the "canals" or "human faces" on Mars; they disappeared with better new observations and higher resolution (S2: slide #25). The adequate GR of the gravity model is an important, necessary but not sufficient condition and a limiting factor for the correct interpretation of the gravity aspects. The definition of GR is recalled in S2:23 and we can only repeat (Sect. 3) that the GR of EIGEN 6C4 is 9 km but can be enhanced to about 4 km (see above). This provides clear limit for any interpretation. The subglacial topography has a similar problem: data gathered from airplanes over Antarctica (Bedmap 2) are not homogeneous in latitude and longitude, not complete and has large gaps (Fretwell et al., 2013). Taking the resolution of the subglacial topography data Bedmap 2 as published, i.e. net 1x1 km literally, we can get pictures of the topography showing unrealistic shapes instead of real features (Klokočník et al. 2021); the artefacts are looking like walls, pyramids, etc (for example S2: 28). The problem is that the data density is somewhere ~5 km but ~50 km on other localities; there are zones with no data at all. We have to know how well the data has covered the area of our interest (*fig. 3* in Fretwell et al., 2013).

4.3. Signal degradation and truncation error tests

A treacherous situation with artefacts can be demonstrated by using the gravity model to its maximum degree and order d/o in harmonic expansion, exactly as it was published. The result may be surprising. A model is published say to d/o =1200 but recommended to be used (by the authors of the model themselves) only to max d/o = 600. The reason is stabilization of the large matrix inversion by Kaula rule for the higher-degree part of the model. The full model can show a significant graining in the gravity aspects leading to total damage of the signal, see S2 (in all the gravity aspects; faster degradation was observed for the gravity aspects with higher derivatives of the disturbing potential; Klokočník et al., 2021).

Figure S2:29 shows one of our many tests, in this case for the Moon‘s crater Copernicus with the gravity model GRGM1200A (Lemoine et al., 2014) till d/o = 1200. Practically useful limit at d/o ~ 600 corresponds to the theoretical ground resolution ~10 km. This is already comparable to the Earth, to its EIGEN 6C4 gravity model to d/o=2190 (Foerste et al., 2014) because the Moon is smaller than the Earth. When we use GRGM1200A up to d/o=600, we can see a reasonable result S2:29 showing all known features. When we cut at d/o 130, a part of useful signal is lost. When we use the model to d/o=1200, graining is significant and we can interpret nothing.

Let us imagine that today we know the gravity field of the Moon only to d/o=10. What information we lose (or is “hidden“) in a comparison with the full model to d/o=600? Not only the resolution of the former is much lower (expected) but sometimes artefacts are created, look at S2:30 (expected?). Only a further gravity field improvement would eliminate such artefacts. We are now in analogical situation with the gravity field EIGEN 6C4 to d/o=2190 for the Earth. What we would lose and which artefacts might be generated with, say, the model cut at d/o=80? The slides S2: 31, 32 show the result in terms of the strike angles. Often the basic trend in both full model and the cut model is the same, but not always; thanks to the dramatic difference in maximum d/o-used, it must be expected, but in any case, it is a warning. The artefacts “lurk“ and can eventually hamper our endeavour concerning the geo-interpretations. It is not probable but not excluded even for EIGEN6C4 to 2190; the case of artefacts due to an aliasing of the gravity aspects on Sahara is in *fig. 5a* in Klokočník et al. (2021) and S2: 33 here.

5. Popigai

5.1. Introductory notes and geology

This large, proved, exposed impact crater Popigai/Popigaj is in Russia near Khatanga (Chatanga, port on river), Krasnoyarsk district, Siberia (geodetic latitude and longitude of the centre of the crater: φ=71°36′N and λ=110°55′E). It is a 100-kilometre diameter proper crater ~35 million years old (from the late Eocene epoch). It was considered for the first time as an impact crater by Masaitis et al. (1972), based especially on petrographic observations of the various breccias. It is the largest known impact crater post-dating the Cretaceous–Tertiary boundary (e.g., among many others, Vishnevsky & Montanari, 1999, Whitehead et al., 2000, Koeberl 2009, Masaitis 1998, Masaitis et al., 2019).

The impactor is suggested to have been a H chondrite asteroid several kilometres in diameter (e.g., Schmitz et al., 2015) from the main asteroid belt. The asteroids may have approached the Earth at comparatively low speeds, passed the Roche limit and produced a meteoritic shower. But also a multi-type asteroid shower may have been recorded, triggered by changes of planetary orbital elements due to orbital resonances (see again, e.g., Schmitz et al., 2015). There is no agreement among researchers.

The Popigai crater lies on the eastern edge of the Archean Anabar Shield, which is mainly composed of granitoids and gneisses. It is surrounded by a relatively complex envelope of Precambrian, Paleolozoic and Cenozoic rocks, which reach 1-1.5 km in thickness at the point of impact (Masaitis 1998, Pilkington et al., 2002). It is a multi-ring structure with three concentric rims visible.

The bedrock is crushed to depths of at least 5 km according to the results of drilling and geophysical measurements. The internal structure of the crater is quite unusual and contains a number of enigmatic phenomena, such as the presence of impact breccias fused into glassy, also fragmented tagamites (breccia within breccia). Vishnevsky & Montanari (1999) propose that the contrasting sedimentology or the presence of water in some layers of the original pre-impact sedimentary succession may have triggered a whole chain of impact phenomena. A similar result could be caused by the nearly simultaneous, close impact of two or more meteorite fragments.

The long-term evolving terrains always have a complex tectonic framework, or rather a sequence of tectonic regimes creating a network of faults of different ages and directions. Masaitis (1998) in his diagram of the crater shows radial tectonics in the immediate vicinity of the crater,

while in Vishnevsky & Montanari (1999), long faults of NW-SE and SW-SE directions are displayed. Somewhat unexpectedly, faults in the NS direction predominate in the crater itself, without any apparent influence of the impacting body.

Looking at the broader tectonic framework, we see a number of significant structures based on faults of approximately NS direction. The latter follows the Ural Mountains, the western margin of the Central Siberian Plateau, the Verkhoyansk Chrebet (belt), and some rivers such as the Daldyn River directly in the crater and around parts of the course of the Anabar and Malaya Kuonamka rivers. Perpendicular to them, a long EW structure visible with ETOPO 1 (Fig. 1), is located, north of the crater (see the arrows from E and from W).

The impact's shock pressure instantaneously transformed graphite in the ground into diamonds (e.g., Masaitis et al., 1972, Masaitis 1998, Deutsch et al., 2000). The aggregates of diamonds are sometimes up 1 cm large. They tend to retain the appearance of graphite or original organic aggregates. They are bound to outcrops of original rocks with an admixture of graphite or coal substance. They are absent in the central part of the crater, where the pressure and temperature were too high for diamonds to form or preserve (see, e.g., *fig. 1* in Masaitis 1998). Vishnevsky and Montanari (1999) presented (cf. *fig. 6*, p. 26) a diamond occurrence map showing a more or less chaotic distribution caused by both an irregular admixture of carbon-rich impacted rocks and a complex, multiphase crater evolution. Popigai is most probably linked to ejecta horizons occurring in marine sequences of Late Eocene age.

Pilkington et al. (2002) presented Δg based on the local gravimetric data showing a negative "valley" going from the main and proven Popigai crater in the SE direction (cf. *fig. 3a* in Pilkington et al., 2002) which is an indication of a possibility that we deal with double/multiple craters.

Popigai may be a multiple crater (Klokočník et al., 2010), a catena like on the Moon (Figs. 2a,b and slides #6-21 in S3); it was proposed in Klokočník et al. (2010), based on analysis of Δg and T_{zz} derived from (at that time the best) global gravity field model of the Earth EGM 2008. Popigai may represent one of two or three simultaneous impacts from one original asteroid. Some authors consider asteroid shower from a single parent-body breakup (Schmitz et al., 2015).

Popigai has been designated by UNESCO as part of the world's geological heritage. Due to economic reasons, exploration work in this remote area (the joint German-Canadian-Russian expedition) has ceased before 2000 (according to information from Deutsch et al., 2009).

For completeness of these records, we note that near Popigai, roughly in the SW direction of Popigai, another, not yet proven crater, independent of and bigger than Popigai. This feature, known as Kotuykanskaya, is a hypothetical impact crater. It is located around φ=69°30′N; λ=100°25′E (Rajmon 2009; Klokočník et al. 2020c and references in this paper; also S3: 14-17).

5.2. Our new gravity results for Popigai

The recent global satellite-based surface topography depicted by the ETOPO 1 model is shown in Fig. 1 (and variants in S3). There is a broad topographic low in NE, E, and SE directions from the main Popigai crater. One reckons that the terrain may has been strongly affected by water/ice erosion and other influences since time of the impact event – e.g., a river is flowing throughout the bottom of the crater, the rim is disrupted significantly on two places with consequences on the gravity signal (see reaction in the gravity signal in the following figures).

The structure is characterized by a strong gravity low of Δg = -40mGal and T_{zz} = - 30E amplitude (EIGEN 6C4). Superimposed on the gravity low is a concentric ring-shaped high, which is presently fragmented, possibly due to postimpact evolution. The central peak is well visible, Figs. 2-3, not with too much intensity.

Fig. 2a shows Δg, Fig. 2b presents T_{zz}. Fig. 3 is a zoom just for θ (I<0.9) in the main crater, with a halo of the strike angles; there is a signature of the central peak, too. The topography (Fig. 1) and the gravity aspects (Figs. 2-3 and S3) do not correlate.

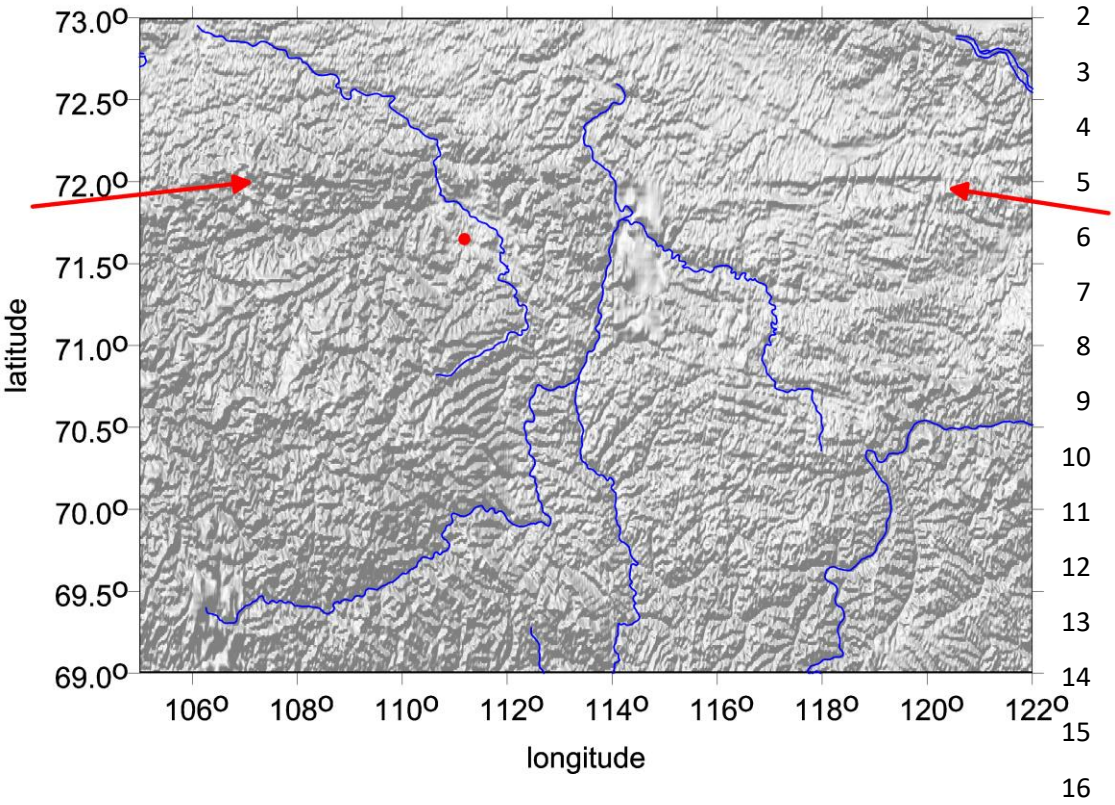

Fig. 1. Popigai: ETOPO 1 topography [m], shaded relief; red dot means the crater's centre; an alternative projection, with contour lines, is in S3. The arrows show EW going linear structure; its gravity signal is weak.

(a) (b)

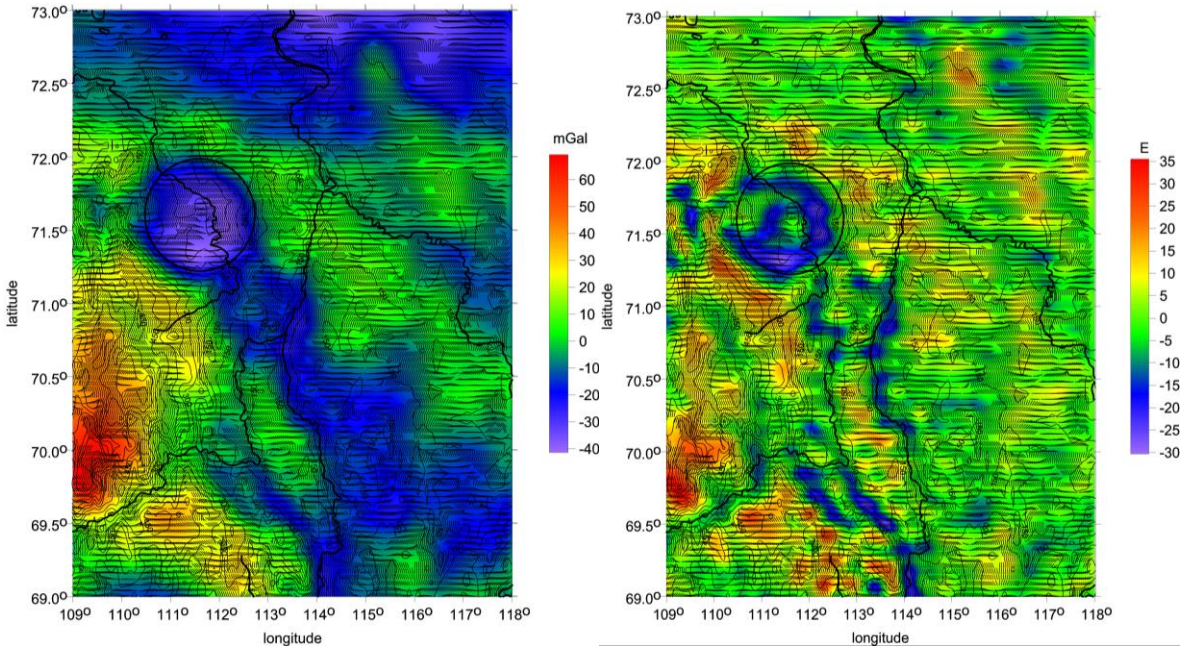

Fig. 2. Popigai: **(a)** Δg [mGal] and θ [deg], $I < 0.9$ with the topography; **(b)** T_{zz} [E], θ, plus the topography from ETOPO 1; topography and gravity do not correlate too much. Technical note: everywhere, cool colours are lows, warm colours are highs, green is for zero. North: everywhere up (meaning in the direction to the present-day north pole of rotation of the Earth and present-day continent positions).

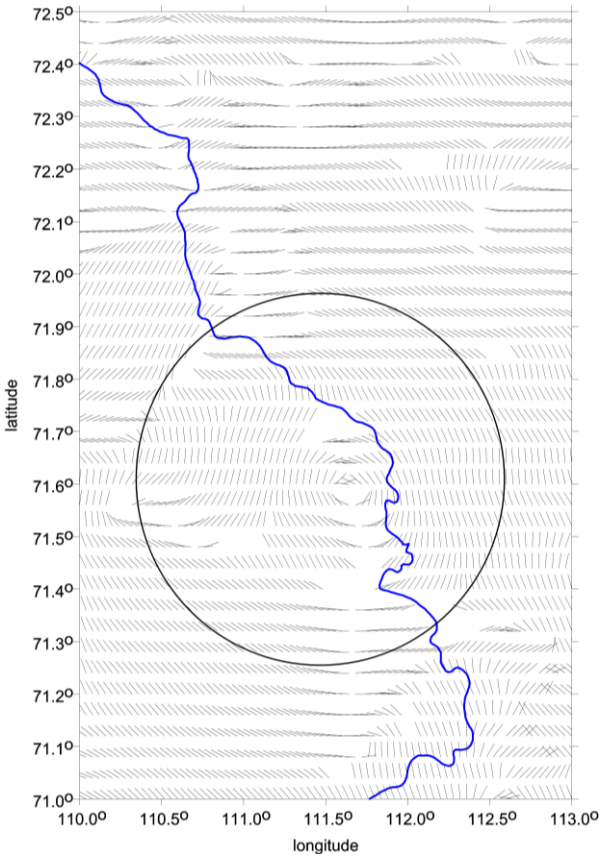

Fig. 3. Popigai: details for θ in the main, largest and proven Popigai crater. The halo of the strike angles combed around the crater bottom (circle) and its central. The Popigai river (in blue) locally disrupts the halo.

Beside the main, proven crater, we clearly see more candidates for impact craters (which are a bit smaller than the main crater). They are aligned in the SE direction (Klokočník et al., 2010, 2020b, Khazanovitch-Wulff et al., 2013). It is obvious from Figs. 2a,b, from broad negative Δg, from negative belts and semicircles of T_{zz}, and from the strike angles θ included in these figures (also S3: 8, 9, 21). These θ have tendency to be directed along the long axis of the whole Popigai family (SE-NW), interrupted only locally inside the potential craters (e.g. S3: 21). We labelled these crater candidates as Popigai II-IV in (Klokočník et al., 2010). Counting from the main and proven Popigai crater (Popigai I), a large circular structure is visible on the SE rim of the main crater. It can be the companion crater – what we called Popigai II in (Klokočník et al., 2010). At that time, we did not have the strike angles and the virtual deformations at our disposal. With them now, we can better demonstrate that Popigai can indeed be a double or multiple crater, i.e. catena, a rare phenomenon on the Earth (the "Popigai family").

6. Chicxulub

6.1. Introductory notes and geology

The impact crater Chicxulub (Northern Yucátan, México) is centred beneath Chicxulub village (φ=21°17′N and λ=89°30′W) near the Progreso port. The crater is huge, not exposed, with a diameter 170-250 km, and about 65 mil years old. This enormous impact represents an external forcing event (of non-terrestrial origin) with far-reaching, global consequences in mass extinction, as is well-known (the KT event).

The Yucátan peninsula is a low-lying limestone platform. The crater is buried under Quaternary carbonate sediments (0.6-1.0 km thick), lying over Tertiary sandstone and volcanic rocks. The northern (nearly)-half of the now-buried crater is in shallow waters of the Sea of Campeche (of Gulf of Mexico), which then falls, at the northern end of the Campeche Bank, to deeps in the Campeche Escarpment (fault).

The origin of the impactor in the Solar System is not yet clear. Bottke et al. (2007) proposed that the Chicxulub impactor could have originated from a moderately young asteroid family Baptistina. Located in the inner main belt of asteroids, this cluster is favourably positioned to deliver large objects (>5 km) to the terrestrial planets. A recent analysis of Nesvorný et al (2021) claims that the crater was produced by impact of a carbonaceous chondrite and suggest that the impactor came from a main belt asteroid that quite likely ($\simeq$ 60% probability) originated beyond 2.5 au. Some authors discuss about a comet as the impactor (e.g., Desch et al., 2021; now minority opinion); the comet would become from the Oort cloud. The impactor might be also a binary asteroid, but it is rare (as we know) to produce two craters with two asteroids. The asteroids must be sufficiently separated (s/c “wide binaries”). Two closer impactors can produce one crater, one elongated crater, or two overlapping craters (Miljikovic et al., 2013).

The impactor’s direction has been studied, among others, by Hildebrand et al. (2003). We quote: „the impact direction was towards the northeast based on the asymmetries preserved in various of Chicxulub’s structural elements in addition to the vergence observed in the central uplift: compressional structures outside the crater rim, the rim uplift, compressional deformation preserved in the slumped blocks, morphology of the peak ring, off centre position of the central

uplift in the collapsed disruption cavity (CDC), elongated CDC, and initiation of slumping of Cretaceous stratigraphy off the Yucatan platform."

The literature about the Chicxulub crater is really rich. To mention a few: Alvarez et al. (1979, 1980); Smit & Hertogen (1980); Hildebrand et al. (1990, 1995); Ramos (1975), Campos-Enriquez et al. (2004), Gulick et al. (2008, 2016); Goderis et al. (2021) or Urrutia-Fucugauchi et al. (2022). We recall the important role of terrestrial gravity data in its study. Already Hildebrand et al (1998) used not only the terrestrial gravity anomalies (measured for oil/gas prospection) but also horizontal second derivatives to enhance resolution; but were not aware of the concept of gravity aspects. According to Klokočník et al. (2010), Chicxulub may be a double crater; it was suggested after the analysis of Δg and T_{zz} based on EGM 2008 (compare with *fig. 2* in Hildebrand et al., 2003).

Strong impacts like this one have global effects; regionally enormous pressure can trigger many postimpact activities and features. Let us recall Donofrio (1998) who wrote: "Seventeen confirmed impact structures occur in petroliferous area of North America, nine of which are being exploited for commercial hydrocarbons… Disrupted rocks in proximity to impact structures, such as Chicxulub in the Gulf of Mexico off Yucatan, also contain hydrocarbon deposits". James et al (2002), p. 40, wrote: "…There are several craters that host fossil fuels, with the submarine Chicxulub impact crater…" and "…a total of 21 craters have oil/gas/hydrocarbon/coal resources, of which 19 host oil and gas." The reader can see slides #17-18 in S4.

A rapid burial of Chicxulub by Cenozoic sediments contributes to its preservation but also limits its study. The direct, surficial or submarine geological study of Chicxulub is impossible because the structure is buried by several hundred metres to 1 km of porous Tertiary limestones (Ramos 1975). A 2016 drilling project revealed a central ring composed of originally deep-seated, coarse-grained granite (Morgan et al., 2016). It is important because analogously we can expect rocks from depths of >10 km in, for example, lunar craters, as Kring (2016) reports for the crater Schrödinger. The concentric structure of Chicxulub is surrounded by the ring of cenotes. It indicates finely fractured, and more permeable zones, on those the extensive cave systems developed. At the surface it manifests as cenotes i.e. collapsed cave ceilings (Perry et al. 1995). In a wider surrounding, the karst phenomena are known on the north-eastern margin of the Yucatan in the Holbox tectonic zone, but here they are much more likely connected to the broad active arc

that encircles Cuba from the north and trends toward the Yucatan (the Pinar Zone and Oriente Fault Zone).

6.2. Our new gravity results for Chicxulub

The gravity anomalies around Chicxulub are shown in Figs. 5-7, the radial component T_{zz} in S4:21, T_{xx}, T_{yy}, T_{zz} in S4:22, the invariants I_1, I_2 in S4:23, their ratio I in S4: 24, and vd in Fig. 8 and S4: 24, 26, 27. The strike angles θ are in S4:25; they are also underlying several other figures with the gravity aspects. We do not forget on the ring of cenotes (sinkholes, originally potable water sources used by Maya; S4: 9-11, 27, and 31).

The surface topography ETOPO 1 (Fig 4) does not correlate with the gravity aspects (the crater is not visible on the surface); even Ticul Fault and Ticul Sierra (hills) do not correlate with gravity.

We can see the positive T_{zz} at the central peak and along the rims, negative T_{zz} in between the rings. The strike angles are combed inside the crater, clearly laid down along the rims (analogy to Vredefort, S2: 9), so they correlate also with the ring of cenotes (S4: 10). Outside the central crater, the prevailing direction is SW to SE. The strike angles, combed around Chicxulub to halos, following the craters' rims, are conspicuous on land. The ring of cenotes agrees well with the halo created by the strike angles along the outer, most compact ring of the crater. Cenotes then continue like a cluster on the east edge of the crater (S2: 9). Good to note that with the gravity aspects we can register the effect of all cenotes together, not the individual features, of course.

Tertiary sedimentary layers of the flat northern Yucatan outside the crater have, as expected, linear and also highly combed θ. A contrast of the density of sediment or a changed porosity (with respect to surrounding rocks) is high enough to be gravitationally distinguishable. The cenotes as well as oil/gas deposits near Yucatan, although epigenetic, are not there by a chance (e.g., Grieve 2005, p. 21) but as a consequence, direct or indirect, of the impact event.

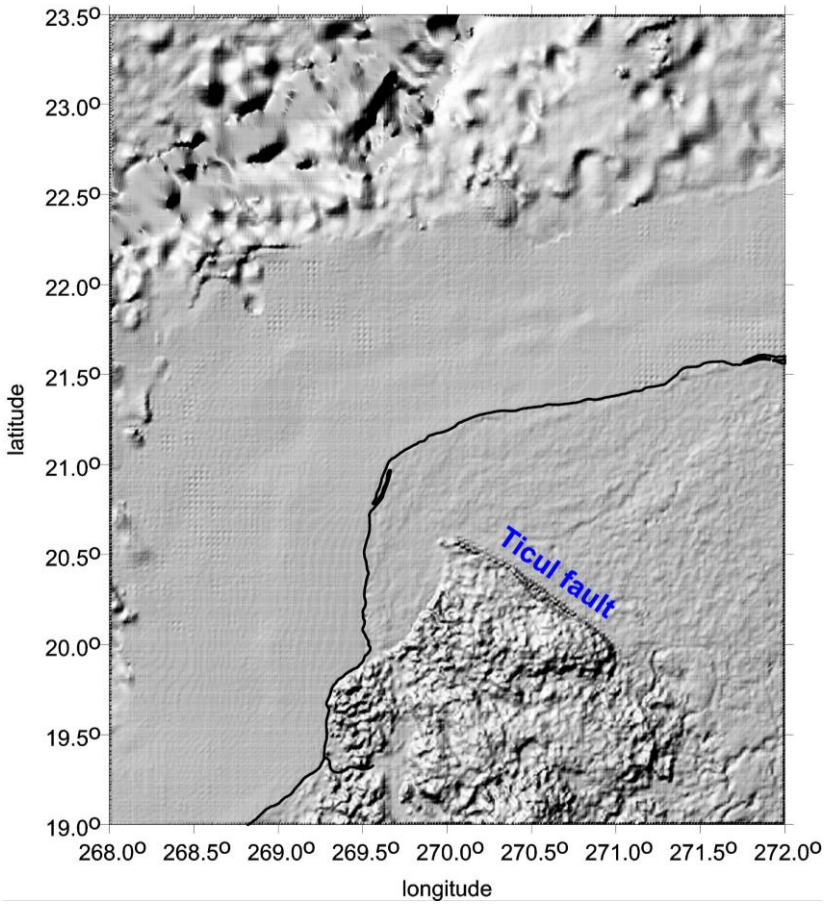

Fig. 4. Northern Yucátan, México, flat low-land and shallow-sea area of the buried Chicxulub impact crater, ETOPO 1 topography (without any gravity aspect added) in an enhanced shaded relief scale (compare to S4: 8-10, 26). Tertiary sediments cover the impact crater; only semi-circular "shadows" NE of Ticul fault, due to the cenote rings, are visible in the plain terrain (here and in S4: 8). Black line: the coast.

Our figures demonstrate a halo around the central part (min. two rings). The strike angles are also strongly linearly combed far from the crater, mainly SW NE (due to the local high porosity around and the cenotes outside the rims of Chicxulub E of them).

Fig. 8 presents the virtual deformations (*vd*), red for dilatation, blue for compression. The *vd* perfectly depict the bottom of the crater, its central peak, the rings, and the combed areas around.

We newly analysed the negative "southern gravity anomaly" (located S to SW of the main crater) in the NS direction; we call this feature the "tail", see Figs. 5-7, S4: 15-17, 25, and 26. The prevailing, standard opinion is that this is a pre-impact feature (e.g., Gulick et al., 2008; Urrutia-Fucugauchi et al., 2022).

The tail or trench-like structure or NS elongated depression of the graben type has a negative gravity anomaly. Linearly combed strike angles in the same direction (Fig. 5-6 and S4) indicate syngenetic feature with the impact crater(s). The *vd* in Fig. 8 show the best the whole linear feature, the hypothetical impact graben, connected with the impact craters. The southern tail would be its southern end.

This tail is replicated in the younger relief uplifted SW of the Ticul fault (see ETOPO 1 morphology, Fig. 4). Extending the trench axis southward (Fig. 5), another linear depression (dark and light green) is encountered in a nearly perpendicular direction, trending northward and forming a "V" like shape. For both these structures, we suggest that the influence of the impact on pre-existing geological structures may have been at work.

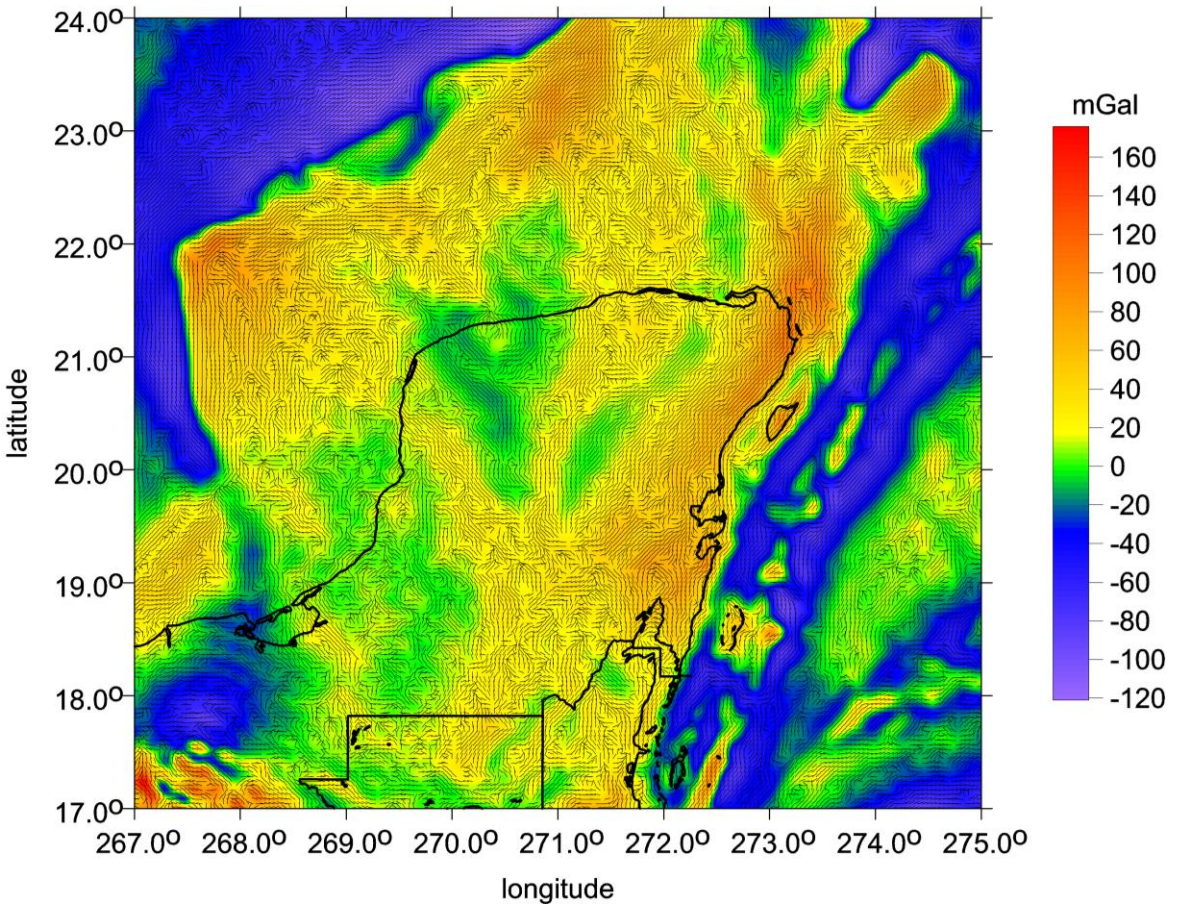

Fig. 5. Northern Yucátan, México, the area of Chicxulub impact crater, using the gravity model EIGEN 6C4 to maximum degree and order d/o=2190, with a 4 km resolution. The gravity anomalies Δg [mGal], together with the gravity strike angles θ [deg], I <0.9. Black lines: coast and state borders. The strike angles as a parameter of the gravity anisotropy tensor $\mathbf{\Gamma}$ reveal up to three ringed structures of the Chicxulub basin. The combed strike angles correlate with oil/gas deposits (it continues to SW to Campeche off-shore oil fields), also with its rims and with a (semi)ring of the cenotes (on land). These are sinkholes (karst features) in the local limestone sediments; they were used by Maya as a source of drinkable water. They represent one of the post-impact effects. The second radial derivative T_{zz} and other gravity aspects (including the combed strike angles with the *Comb* statistics) are shown in S4:25.

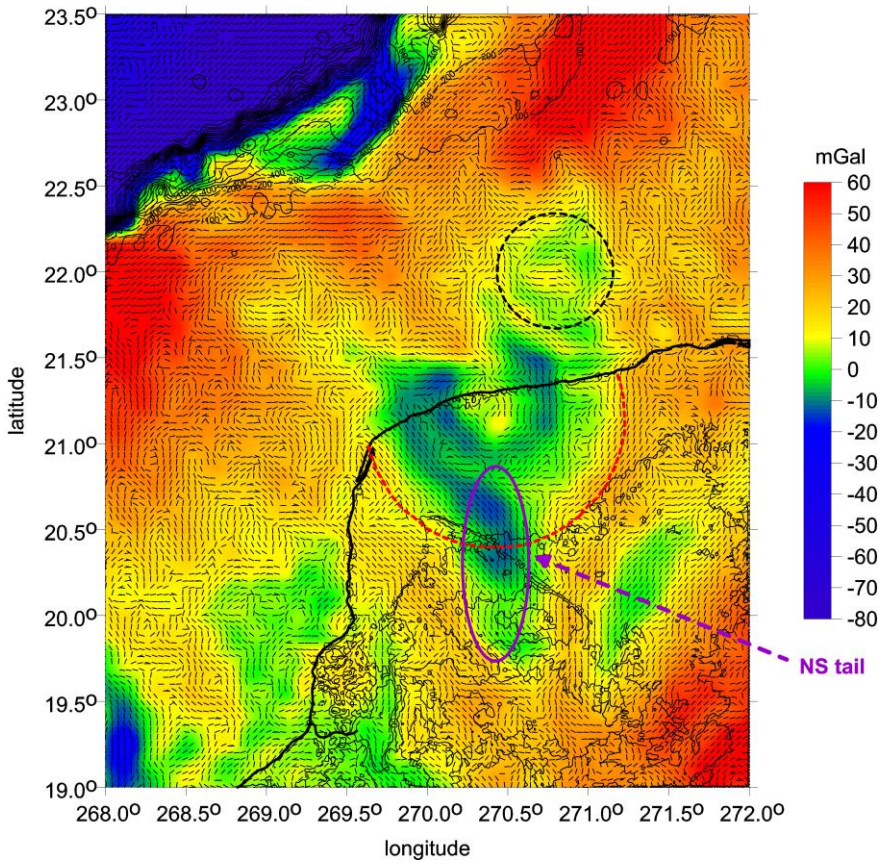

Fig. 6. Gravity anomalies Δ*g* (complete EIGEN 6C4 to d/o=2190) [mGal] and strike angles [deg] with ETOPO1 topography. *Circles* for Chicxulub I (proven) and II (hypothetical) impact craters; the *ellipse* for the NS elongated depression of graben type (the „tail“), a part of the impact event.

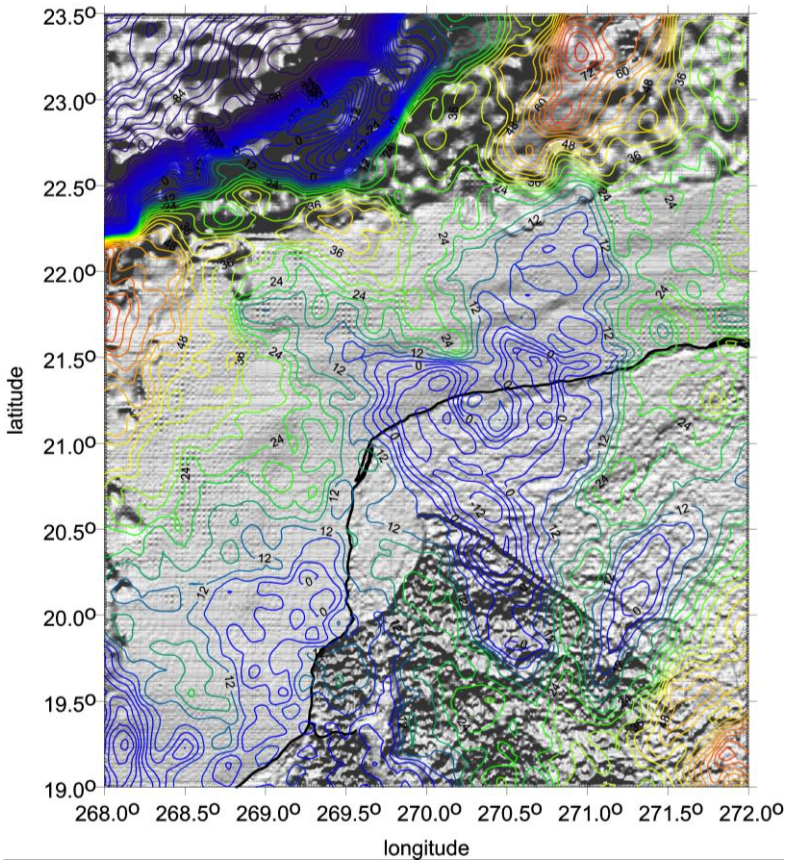

Fig. 7. Gravity anomalies (full EIGEN 6C4) [mGal] as contour lines and the ETOPO 1 topography as shaded relief. For more figures see S4: 5, 11, 12, 19, 20, and 28. Negative Δg values are in blue colour.

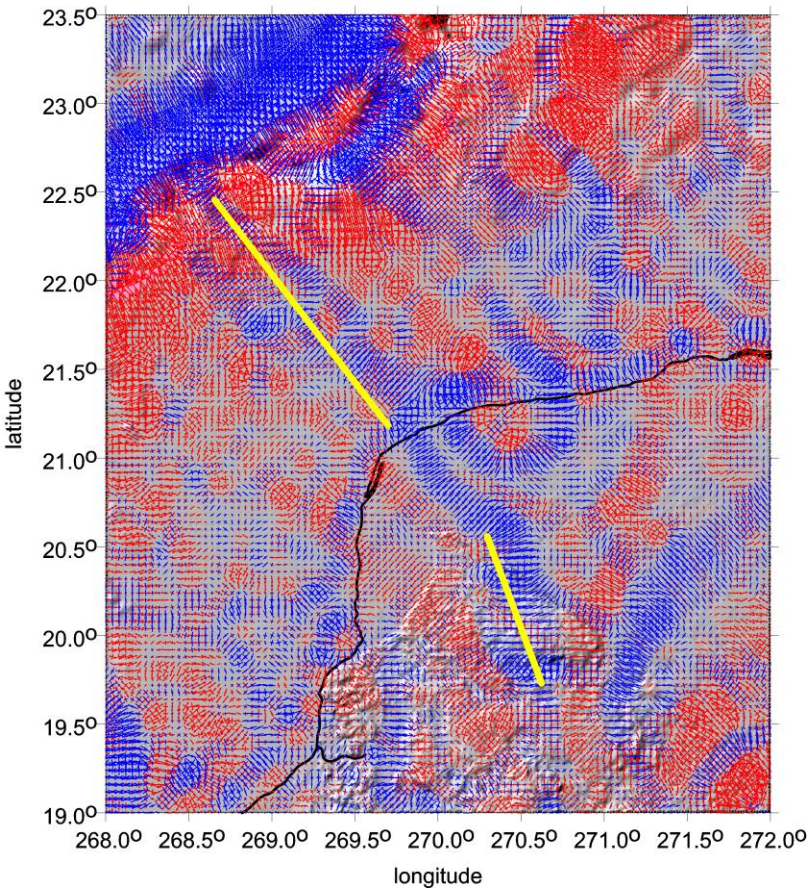

Fig. 8. The virtual deformations *vd* [-] (compression in blue, dilatation in red) with EIGEN 6C4 in 4 km grid. Black line: the coast. *Yellow lines:* hypothetical impact graben including a „tail" roughly in the NS direction.

7. Discussion

Popigai

1. Beside the main, proven crater, we clearly see more candidates for the impact craters; they are lined in the NW-SE direction (as we observed in Klokočník et al., 2010 and denoted them there Popigai II, III, and IV). Here we confirm these our previous findings (Figs. 2-3 and S3). The area SE of the main crater has negative values of Δg and T_{zz}, and aligned strike angles θ.
2. Topography (ETOPO 1) and the gravity aspects do not correlate well. This indicates a partial smoothing of the impact features by erosion and filling of the impact-made depressions, in this case of both craters (including the hypothetical Popigai II crater) and the hypothetical in the NW to SE direction running impact trench.

3. The strike angles are combed into a halo around the main, proven crater Popigai I and are partly overlapping with the aligned but fragmented strike angles for Popigai II (Figs. 2a,b and S3).
4. A long, EW oriented structure, visible with ETOPO 1 (Fig. 1) and with the gravity aspects (Figs. 2a,b) is located north of the main crater Popigai I (see the arrows at Fig. 1). We have mentioned in Sect. 5.1. that unexpectedly the NS faults dominate in the crater without any apparent influence of the impacting body (Masaitis 2008), while other tectonic schemes (Mashchak & Naumov 2005) found the evidence of the expected radial tectonics. Masaitis (1998) in his diagram of the crater shows radial tectonics in the immediate vicinity of the crater, In Vishnevsky & Montanari (1999), however, long faults of NW-SE and SW-SE directions are displayed.

The NW-SE linear structure connecting the craters is of particular interest to us because in the SE from Popigai I we can observe a long and wide depression to the distance of ~400 km (Figs. 2a,b). This type of image is repeatedly encountered in most geological interpretations of the gravity data, typically, e.g., for the ancient Nile valleys or lake basins covered, e.g., by Saharan aeolian sands, or hidden under the Antarctic glaciers. We therefore assume that a depression filled with younger sediments extends south of the Popigai craters. According to analogies with other terrestrial structures, the thickness of the fill could be 1 km or more.

5. Given the close spatial association of the circular impact structure (the crater) to the linear NW-SE running "basin", we guess the linear feature can be original tectonic belt that was reactivated in extensional mode after the impact and subsequently filled with sediments in a dynamically evolving Cenozoic landscape. It could be formed or influenced by Neogene movements related to the Tethys belt, but also to the periglacial regime of the Siberian North. Long-term evolving terrains always have a complex tectonic framework, or rather a sequence of tectonic regimes creating a network of faults of different ages and orientations.

Looking at the broader tectonic framework, one can see a number of significant structures based on faults of roughly NS or NW to SE direction. It follows the Ural Mountains, the western margin of the Central Siberian Plateau, the Verkhoyansk Chrebet, and other rivers such as the Daldyn River directly in the crater and around. The NW-SE linear depression resembles an impact graben, i.e. a "trench modified by impact". The heart of an impact graben is a pre-impact geological structure, activated by the impact energy to form a graben. This is not a new concept, as we observe basaltic rock eruptions in the extensional pressure regime in impacts on the Moon and Mars (e.g.,

Wichman 1993, Spudis 1993, Dasgupta et al., 2019, Zhang et al., 2023) or in some large terrestrial craters (Sudbury). In contrast, in the compressional tectonic regime, impact horsts are formed, such as those observed on the uplifted crater rims. The two stress-release or compression-extension regimes are complementary, usually perpendicular or oblique to each other. Especially in inhomogeneous terrestrial conditions (except perhaps in stable Archean blocks), meteorites strike areas with already existing regional stress fields. The stresses are then activated in specific directions by the enormous kinetic energy of the impactor.

Mashak and Naumov (2005) stated: "…Thus, the 35-Ma-long post-impact modification history of the Popigai crater is determined by the superimposition of the regional tectonics on the long-term relaxation movements. As a whole, the late modification stage tectonics is found to have only an insignificant effect to the Popigai crater, so that both the original structure and the crater topography have been retained in a good state." The existence of circular structure Popigai II and closely associated trench evokes the possibility of almost concurrent formation of impact crater (or craters) and impact NW-SE oriented graben.

Chicxulub

1. Topography (ETOPO 1) and the gravity aspects (namely Δg, T_{zz}, vd, and the invariants) do not correlate.
2. The majority of cenotes agree with the innermost ring (or the second ring, when counting the central ring around the central peak as the first ring) having positive Δg, T_{zz} and strike angles combed into a halo.
3. The “southern tail” with negative Δg and T_{zz} and with the strike angles θ, aligned in the SN direction, seems to be an inseparable part of one impact event (this impact may consist of several explosions). The strike angles, continuing from the main crater from its halo to south, have a stream flowing from the halo to the SN tail, changing slowly its direction from NW-SE to NS; it is looking like one common feature (the crater and the tail together).
4. Besides the main, proved crater, we have predicted earlier (in Klokočník et al., 2010) another smaller crater in NE direction. Accounting for all new gravity aspects, this still remains possible (see circle in Fig. 6). Moreover, after a careful inspection, one can distinguish several more, small circular features (in Fig. 5) near the Chicxulub crater (namely SW of it),

which might be also impact craters, scattered around the primary. But this is just a speculation.

Christensen et al. (2009) and others argued that the gravity signal near Chicxulub is associated rather with pre-existing Cretaceous basin proposed for this location (Gulick et al., 2008) than with additional crater(s). Our tools (Δg and T_{zz}) and EGM2008 (predecessor of EIGEN6C4) in 2010 were not sufficient to solve the problem. Moreover, we always wish to rely upon additional geological, geophysical, and other data, when available. In the meantime, with the gravity aspects, our tools improved and our experience with the gravity aspects increased. It is specifically the strike angle θ that proved to be very inspiring for diverse geoapplications in the case that stresses are present. The combed strike angles around Chicxulub create a halo (which is expected and usual phenomenon for the impact craters and basins, similarly as on the Moon or Mars), from which on its south side, a flow of θ is changing its direction to south. There is no interruption, no jump, no separation as we should observe between two separate geological features, telling us that the crater itself and its southern tail belong to one and the same body.

Previous studies have suggested assymetries in the Chicxulub crater (e.g. Hildebrand et al., 2003; Gulick et al., 2008). This might be used to estimate the direction of impactor in the atmosphere. However, seismic data show significant variations on the composition of the target rocks around the impact site. It is unclear as to whether the angle of impact or target material heterogeneity is responsible for the asymmetry (e.g., Collins et al., 2008).

Similarly, as for the Popigai family, we are interested in the linear structures near Chicxulub, namely in a trench-like structure running NW-SE of the main Chicxulub crater (Fig. 8). It is replicated in younger relief uplifted SW of the Ticul fault (see ETOPO morphology. Fig. 4). Extending the trench axis southward in Fig. 5, another linear depression (dark and light green) is encountered in a nearly perpendicular direction, trending northward and forming a "V" like shape. For both of these structures, we suggest that a reviving influence of the impact on the pre-existing geological structures may have been at work.

Similarly to the Popigai crater family in Figs. 1-3, we can see here in Figs. 4-8 how the circular impact structure is followed by a tectonic trench. In both craters, its direction roughly corresponds to the orientation of the surrounding geological structures. Thus, we assume that the faults, fault zones or generally weakened structures already existed in these places before the impact. According to the gravity aspects, where the crater and the adjacent trench have a similar signal,

we believe that the impact activated these structures form what we call an impact graben. However, both craters were rapidly filled with younger sediments, thus burying both the circular impact structure and the linear trenches.

Another interesting view is offered by Fig. 8, which shows the virtual deformation. Let us focus on the broad, blue lines that emanate from both arms of the crater to the NW. At the easternmost line, we observe a continuation along the shelf towards the edge of the continental slope, giving the impression of a valley formed on some impact-weakened zone. The western (blue marked) zone is much longer, partially overlapping with the structures shown earlier (see Figs. 5-7).

For both crater formations, we consider the existence and a relationship between their circular (crater) and linear components (graben-like structures). However, there is a different post-impact geological evolution for the linear trench-like structures, as they naturally become erosional pathways and as such, they are subject to both down cutting into the bedrock and filling with younger sediments, in different ways in both locations (Siberia, Yucatan).

Astronomical note: The gravity aspects cannot themselves decide whether the impactor was a single body or a binary asteroid before its impact on the Earth. Both is possible. As noted above (Sect. 5.1.), there is a possibility of break-up of one body (a single asteroid) in the atmosphere or a "flying cluster" of bodies encountering the atmosphere or wide binaries. To create a double crater, components of a binary asteroid must have a big distance, or in other words, a large separation (hundred kilometres). These are s/c wide binaries in a contrast to close binaries. Velocity of asteroids in the Solar System is much higher than velocity of a point rotating on the Earth's surface. Thus, close binary asteroids can quickly hit one place twice and create one crater only.

As for the direction of the impactor: sometimes we can deduce this direction from the strike angles (Klokočník et al., 2020b), looking at how they are combed. As a good guide, we offer Steinheim-Ries (S2:18). Geologists know that the impactor(s) came roughly from W, creating first the smaller Steinheim, than the bigger Ries. We can verify it independently using the strike angles; they are combed in the ~WE direction, they are skirting around both craters, creating a fragmented halo around Ries (disturbed by post-impact activities). For Popigai, we can expect impactor coming from ES to NW, producing the small(er) crater(s) and finally the biggest, already proven one (Figs. 2-3, S3:6-21).

Geological note: For the Popigai family, the gravity aspects decoded an arrangement of two or more possible craters in a line, which evokes a lunar catena. Smaller craters will have a weak and fragmented gravity record or they may have disappeared due to postimpact processes. For Chicxulub, our results admit existence of two craters (Fig. 6). Boreholes to the bottom of a shallow sea north of the NW Yucatan peninsula are known but not on the places where we would need them for the test of the second, smaller, unproven crater. More boreholes and seismic profiles at specific localities (Fig. 6) might clarify the situation (S4:32).

8. Conclusion

We confirm and extend our results from Klokočník et al. (2010) which were based on analysis of Δg and T_{zz} derived from the gravity model EGM2008. Now we work the gravity aspects (including those Δg and T_{zz}) and with the EIGEN 6C4 model. Thus, we have (in comparison with 2010) better tools (the set of the gravity aspects) and better model (EIGEN6C4, with global gradiometric GOCE data). In turn, we are able to support or reject our older results with a higher reliability, with more weight. The result is that we argue in favour of double/multiple craters – and bring further findings.

The impact affects or creates not only the circular structures but also other accompanying phenomena. These may be oriented concentrically as the cenote belts, but also as linear trenches suggesting the existence of the impact grabens. Their orientation and course depend on the regional tectonic architecture and stress fields prevailing at the time of the impact event and after it.

Popigai (Figs. 1-3) is probably a multiple crater, catena (the smaller craters are located SE of the main, proven crater). We consider at least Popigai II as proved crater by our new method and data. SE-NW is the probable direction of the impactor. The broad and long negative gravity anomaly in SE direction of the main crater Popigai I indicates a close coupling between the circular impact structure and a linear depression. They are two possibilities: 1. The depression was formed by reactivation of older geological structures and is the impact graben. 2. The circular structure adjacent to the Popigai I crater in SW gives impression of another, perhaps shallower and more erosion-smoothed impact crater, Popigai II. The gravity aspects at least partially suggest the possibility of a phenomenon that is uncommon on the Earth -– the impact graben may actually represent a catena.

Chicxulub (Figs. 4-8) is probably a double crater; the smaller crater is located NE of the main, proven crater. NE-SW is the probable direction of the impactor. The southern negative anomaly

(the tail) belongs to the impact, as clearly demonstrated by the alignments of the strike angles and changes in their direction. The strike angles are combed into halos around the main crater (typical situation for all bigger impact craters) but then, on the southern side of Chicxulub I, they turn to south (creating the tail). This tail can be the most southern end of the impact graben (Fig. 8) running NW, W to SW of Chicxulub I in the NW-SE direction.

Keywords: impact craters Popigai, Chicxulub – gravity aspects with EIGEN6C4 – gravity strike angles – multiple craters – impact grabens
Funding. This work was supported from the projects RVO: 67985815 and RVO: 67985831 (Czech Academy of Sciences, Czech Republic).
Declaration of interests. The authors declare that they have no competing interests.
Code/Data availability. The gravity field parameters of EIGEN6C4 and ETOPO are generic. Our gravity aspects, computed and plotted by our software, are available on request.
Author contributions. All the authors contributed to the data analyses, writing the manuscript, the discussion and interpretation. Figures were plotted by *surfer* software by Jan Kostelecký.

Appendix/Supplements. Supplementary data to this article can be found online at https://www.asu.cas.cz/~jklokocn/Popigai_Chicxulub_2024_supplements/.

References

Alvarez, W., Alvarez, L., Asaro, F., Michel, H.V. 1979. Anomalous iridium levels at the Cretaceous/Tertiary boundary at Gubbio, Italy: Negative results of tests for a supernova origin. In Christensen, W.K.; Birkelund, T. (eds.). *Cretaceous/Tertiary Boundary Events Symposium*. Vol. 2. Univ. Copenhagen, Denmark. p. 69

Alvarez, L., Alvarez, W., Asaro, F., Michel, H.V. 1980. Extraterrestrial cause for the Cretaceous-Tertiary extinction. *Science* **208** (4408), 1095–1108; DOI:10.1126/science.208.4448.1095; ISSN 0036-8075

Amante, C., Eakins, B.W. 2009. ETOPO1, 1 arc-minute global relief model: procedures, data sources and analysis. *NOAA TM, NESDIS NGDC* 24 (Nat. Geophys. Data Center); DOI:10.7289/V5C8276M

Beiki, M., Pedersen, L. B. 2010. Eigenvector analysis of gravity gradient tensor to locate geologic bodies. *Geophysics*, **75**, 137-149; DOI: 10.1190/1.3484098

Bottke, W.F., Vokrouhlický D., Nesvorný, D. 2007. An asteroid breakup 160 Myr ago as the probable source of the K/T impactor . *Nature.* **449** (7158): 23–25. DOI:10.1038/nature06070

Bucha B., Janák J. 2013. A MATLAB-based graphical user interface program for computing functionals of the geopotential up to ultra-high degrees and orders, *Computers and Geosciences*, **56**, 186-196; DOI: 10.1016/j.cageo.2013.03.012

Campos-Enriquez, J. O. et al. 2004. Shallow crustal structure of Chicxulub impact crater imaged with seismic, gravity and magnetotelluric data: inferences about the central uplift. *Geophys. J. Int.* **157,** 515–525; DOI: 10.1111/j.1365-246X.2004.02243.x

Christeson, G. L., Collins, G. S., Morgan, J. V., Gulick, S. P. S., Barton, P. J., and Warner M. R.: Mantle deformation beneath the Chicxulub impact crater, *Earth Planet. Sci. Lett.,* **284**, 249–257. DOI: 10.1016/j.epsl.2009.04.033, 2009.

Gulick, S. P. S., Barton, P. J., Christeson, G. L., Morgan, J. V., McDonald, M., Mendoza-Cervantes, K.,

Pearson, Z. F., Surendra, A., Urrutia-Fucugauchi, J., Vermeesch, P. M., Warner, M. R.: 2008. Importance of pre-impact crustal structure for the asymmetry of the Chicxulub impact crater, *Nat. Geosci*., **1**, 131–135; DOI:10.1038/ngeo103

Gulick, S., and the Expedition 364 scientists IODP, 2016. Chicxulub: drilling the K-Pg impact crater In collaboration with the International Continental Scientific Drilling Program Platform operations, Onshore Science Party, 21Sept–15 Oct 2016

Goossens, S., Smith, D.E. 2023. Gravity degree–depth relationship using point mass spherical, *Geophys. J. Int*. (2023) **233**, 1878–1889; https://doi.org/10.1093/gji/ggad036

Chodas P. W., Yeomans D. K. 1996. The Orbital Motion and Impact Circumstances of Comet Shoemaker–Levy 9, in *The Collision of Comet Shoemaker–Levy 9 and Jupiter*, Eds. K. S. Noll, P. D. Feldman, and H. A. Weaver, Cambridge University Press, pp. 1–30

Dasgupta, D., Kundu, A., De, K., Dasgupta, N. 2019. Polygonal impact craters in the Thaumasia Minor, Mars: role of pre-existing faults in their formation. *J. Indian Soc. Remote Sens*. **47**, 257-265

Desch, S., Jackson, A., Noviello, J., Anbar, A. 2021. The Chicxulub impactor: comet or asteroid? *Astronomy & Geophysics* **62** (3): 3.34. DOI:10.1093/astrogeo/atab069

Deutsch, A., Masaitis, V.L., Langenhorst, Grieve, R.A.F. 2000. Popigai, Siberia—well preserved giant impact structure, national treasury, and world's geological heritage. *Episodes* **23** (1): 3–12. DOI: 10.18814/epiiugs/2000/v23i1/002

Förste Ch., Bruinsma S., Abrykosov O., Lemoine J-M. et al. 2014. The latest combined global gravity field model including GOCE data up to degree and order 2190 of GFZ Potsdam and GRGS Toulouse (EIGEN 6C4). 5th GOCE user workshop, Paris 25–28, Nov.

French, B. M., Koeberl, C. 2010. The convincing identification of terrestrial meteorite impact structures: what works, what doesn't, and why, *Earth Sci. Rev*., **98** (1–2), 23-170

Fretwell, P., Pritchard, H., Vaughan, D., Bamber, J. et al. 2013. *Bedmap2*: improved ice bed, surface and thickness datasets for Antarctica. *The Cryosphere* **7**, 375–393; DOI: 10.5194/tc-7-37

Hildebrandt, A. R. et al. 1998. Mapping Chixculub crater structure with gravity and seismic reflection data, in *Meteorites: Flux with Time and Impact Effects* (eds). Grady M. M. et al., Geolog. Soc. London, *Spec. Publ*. **140**, 155-176

Hildebrand, A. R., Millar, J.D., Pilkington, M., Lawton, D. 2003. Chicxulub Crater Structure Revealed by 3D Gravity Field Modelling; Conference: *3rd Int. Conf. On Large Meteorite Impacts*, Nordlingen, Germany

Hirt, Ch., Rexer, M., Scheinert, M., Pail, R., Claessens, S., Holmes, S. 2016. A new degree-2190 (10 km resolution) gravity field model for Antarctica developed from GRACE, GOCE and Bedmap 2 data, *J. Geod*. **90**, 105–127; DOI 10:1007/s00190-015-0857-6

James S., Chandran S., Santosh M., Pradeepkumar A. P., Praveen M. N., Sajinkumar K. S. 2002. Meteorite impact craters as hotspots for mineral resources and energy fuels: A global review. *Energy Geoscience* **3**, 2, 136-146

Khazanovitch-Wulff K. M., Mikheeva V., Kuznetsov V. F. 2013. Structural elements of some astroblemes indicating direction of cosmic body trajectories, *New Concepts in Global Tectonics* **1**, 3, 11-18, ISSN 2202-0039

Klokočník J., Kostelecký J., Pešek I., Novák P., Wagner C.A., Sebera J. 2010. Candidates for multiple impact craters?: Popigai and Chicxulub as seen by the global high resolution gravitational field model EGM08, *Solid Earth EGU* **1**, 71-83; DOI: 10.5194/se-1-71-2010. See also: Is Chicxulub a double impact crater? *6th EGU A. von Humboldt Interntl. Conf. on Climate Change, Natural Hazards, and Societies*, Mérida, México, Section: The Cretaceous/Tertiary Boundary and the Chicxulub Impact Crater, paper AvH6-5, 15 March 2010

Klokočník, J., Kostelecký, J. 2015. Gravity signal at Ghawar, Saudi Arabia, from the global gravitational field model EGM 2008 and similarities around, *Arab. J. Geosciences* (Springer-Verlag) **8**: 3515–3522; DOI: 10.1007/s12517-014-1491-y; ISSN 1866-7511

Klokočník, J., Kostelecký, J., Bezděk, A. 2017. *Gravitational Atlas of Antarctica*. Springer Geophysics, ISBN 978-3-319-56639-9

Klokočník, J., Kostelecký, J., Bezděk, A. 2018. On the detection of the Wilkes Land impact crater, *Earth, Planets and Space* 70, 135-147; https://doi.org/10.1186/s40623-018-0904-7

Klokočník, J., Kostelecký, J., Cílek, V., Bezděk, A. 2020a. *Subglacial and underground structures detected from recent gravito-topography data*. Cambridge SP. ISBN (10): 1-5275-4948-8; ISBN (13): 978-1-5275-4948-7

Klokočník, J., Kostelecký, J., Bezděk, A., Kletetschka, G. 2020b. Gravity strike angles: a new approach and tool to estimate the direction of impactors of meteoritic craters, *Planet. Space Sci*.194 (2020), 105113; https://doi.org/10.1016/j.pss.2020.105113.

Klokočník, J., Kostelecký J., Bezděk, A., Kletetschka, G. 2021. Artefacts in gravity field modelling. *Acta Geodyn. Geomat*. **18**, 4 (204), 511-524; DOI: 10.13168/AGG.2021.0036

Klokočník, J., Kostelecký, J., Cílek, V., Kletetschka, G., Bezděk, A. 2022a. Gravity aspects from a recent gravity field model GRGM1200A of the Moon and analysis of magnetic data. *Icarus* **384**, 115086; https://doi.org/10.1016/j.icarus.2022.115086

Klokočník, J., Kostelecký, J., Cílek, V., Bezděk, A., Kletetschka, G. 2022b. *Atlas of the Gravity and Magnetic Fields of the Moon***.** Springer Geophysics. ISBN: 978-3-031-08867-4; https://doi.org/10.1007/978-3-031-08867-4_2

Klokočník, J. Kletetschka, G., Kostelecký, J., Bezděk, A. 2023a. Gravity aspects for Mars, *Icarus* **406**, 115729; https://doi.org/10.1016/j.icarus.2023.115729

Klokočník, J., Kostelecký, J., Bezděk, A., Cílek, V. 2023b. Hydrocarbons on Mars, *Intrntl. J. Astrobiology* (Cambridge UP) **22 (**6), 696–728; https://doi.org/10.1017/S1473550423000216

Kring, D. 2017: *GSA Today*, v. 27, The Geological Society of America. DOI: 10.1130/GSATG352A.1

Kring, D. et al. 2016. Peak-ring structure and kinematics from a multi-disciplinary study of the Schrödinger impact basin. *Nat. Commun*. **7**, 13161; https://doi.org/10.1038/ncomms13161

Lemoine, F.G., Goossens, S., Sabaka, T.J., Nicholas, J.B., Mazarico, E., Rowlands, D.D., et al. 2014. GRGM900C: A degree 900 lunar gravity model from GRAIL primary and extended mission data, *Geophys. Res. Letts*., 41, 3382– 3389; DOI:10.1002/2014GL060027

Masaitis, V.L., Mikhailov, M.V., Selivanovskaya, T.V., 1972, Popigai Basin . an explosion meteorite crater: *Meteoritics* **7,** 1, 39-46.

Masaitis, V. L., 1998, Popigai crater: Origin and distribution of diamond-bearing impactites: *Meteoritics and Planetary Science* **33,** 349-359

Masaitis V. L. 2003. Obscure-bedded Ejecta Facies from the Popigai Impact Structure, Siberia: Lithological Features and Mode of Origin. In C. Koeberl, et al, (Eds), I*mpact Markers in the Stratigraphic Record,* pp.128-162. Springer Verlag Berlin Heidelberg

Mashchak, M.S., Naumov, M.V. 2005. Late Modification-Stage Tectonic Deformation of the Popigai Impact Structure, Russia. In: Koeberl, C., Henkel, H. (eds) *Impact Tectonics.* Impact Studies. Springer, Berlin, Heidelberg; https://doi.org/10.1007/3-540-27548-7_7

Mashchak, M.S., Masaitis, V.L., Raikhlin, A.I., Selivanovskaya, T.V., Naumov, M.V. 2019. (Ed.) Masaitis V.L. *Popigai Impact Structure and its Diamond-Bearing Rocks, Impact Studies*, Springer AG, Springer Nature; *Nat Commun* **14**, 2892 (2023); https://doi.org/10.1038/s41467-023-38615-1

Maus, S., Barckhausen, U., Berkenbosch, H., Bournas, N., Brozena, and 13 coauthors, 2009. EMAG2: A 2-arcmin resolution Earth Magnetic Anomaly Grid compiled from satellite, airborne, and marine magnetic measurements. *Geochemistry, Geophysics, Geosystems* **10**, Q08005

Mendes, B.D.L., Kontny, A., Poelchau, M., Fischer, L.A., Gaus, K., Dudzisz, K., W.M. Kuipers, B.W.M., Dekkers, M.J. 2023. Peak-ring magnetism: Rock and mineral magnetic properties of the Chicxulub impact crater. *GSA Bulletin* 136 (1-2): 307–328; DOI: https://doi.org/10.1130/B36547.1

Miljikovic, K. et al. 2013. Morphology and population of binary asteroid impact craters, *Earth and Planetary Science Letters* 363, 121-132; https://doi.org/10.1016/j.epsl.2012.12.033

Morgan, J. V. et al. 2016. The formation of peak rings in large impact craters. *Science* **354**, 6314, 878-882. DOI: 10.1126/science.aah6561

Nesvorný, D., Bottke, W.F., March, S. 2021. Dark primitive asteroids account for a large share of K/Pg-scale impacts on the Earth, *Icarus* **368**, 114621; https://doi.org/10.1016/j.icarus.2021.114621

Pavlis, N.K., Holmes, S.A., Kenyon, S.C., Factor, J.K. 2008a. EGM2008: An Overview of its Development and Evaluation, National Geospatial-Intelligence Agency, USA, presented *Gravity, Geoid and Earth Observation*, Chania, Crete, Greece, June 23-27, 2008

Pavlis, N.K., Holmes, S.A., Kenyon, S.C., Factor, J.K. 2008b**.** An Earth Gravitational Model to Degree 2160: EGM2008, *EGU General Assembly*, Vienna, Austria, April 13-18, 2008

Pavlis, N.K., Holmes, S.A., Kenyon, S.C., Factor, J.K. 2012. The Development and Evaluation of the Earth Gravitational Model 2008 (EGM2008), *J. Geophys. Res.* **17**, B04406, DOI: 10.1029/2011JB008916

Perry, E., Marin, L., McClain, J., Velázquez, G. 1995. Ring of Cenotes (sinkholes), north-west Yucatan, Mexico: Its hydrogeologic characteristics and possible association with the Chicxulub impact crater, *Geology* **23**, 1, 17-20

Pilkington, M., Grieve, R. A. F. 1992. The Geophysical Signature of Terrestrial Impact Craters, *Rev. Geophys*. **30**, 161-181.

Pilkington, M., Pesonen, L. J., Grieve, R. A. F. and Masaitis, V. L. 2002. Geophysics and Petrophysics of the Popigai Impact Structure, Siberia; in: Plado J., Pesonen L. J. (Eds.): *Impacts in Precambrian Shields*, Springer-Verlag, pp. 87-107.

Rajmon, D. 2009. *Impact database* 2009.1, http://impacts.rajmon.cz; http://www.passc.net/EarthImpactDatabase/index.html, developed and maintained by the Planetary and Space Science Centre, University of New Brunswick, Canada.

Ramos, E.L. 1975. Geological Summary of the Yucatan Peninsula. Chapter in: Nairn, A.E.M., Stehli, F.G. (Eds), *The Gulf of Mexico and the Caribbean*. Springer, Boston, MA.; https://doi.org/10.1007/978-1-4684-8535-6_7

Sebera, J., Wagner, C. A., Bezděk, A., Klokočník, J.: 2013. Short guide to direct gravitational field modelling with Hotine's equations. *J. Geod.* **87**, 223-238.

Sharpton, V. L., Burke, K., Camargo-Zanoguera, A., Hall, S. A., Lee, D. S., Marin, L. E., Suarez-Reynoso, G., Quezada-Muneton, J. M., Spudis, P. D., Urrutia-Fucugauchi, J. 1993. Chicxulub multiring impact basin: size and other characteristics derived from gravity analysis. *Science* **261**, 1564-1567

Schmitz, B.; Boschi, S., Cronholm, A., Heck, P., Monechi, S.; Montanari, A., Terfelt, F. 2015. Fragments of Late Eocene Earth-impacting asteroids linked to disturbance of asteroid belt, *Earth and Planet. Sci. Letts.* **425**, 77–83. DOI: 10.1016/j.epsl.2015.05.041

Smit, J., Hertogen, J. 1980. An extraterrestrial event at the Cretaceous–Tertiary boundary. *Nature* **285**, 198–200; https://doi.org/10.1038/285198a0

Spudis P.D. 1993. *The Geology of Multiring Impact Basins, The Moon and Other Planets*, Cambridge UP, Cambridge Planetary Science Series; (eds). W. I. Axford, G. E. Hunt, and R. Greeley; ISBN 0 521 26103

Surendra, A. 2004. 3D tomographic imaging of the Chicxulub impact crater, *Lithos Sci. Rep*. **6**: 89-92

Pedersen, B. D., Rasmussen, T. M. 1990. The gradient tensor of potential field anomalies: Some implications on data collection and data processing of maps. *Geophysics* **55,** 1558-1566

Saad A. H. 2006. Understanding gravity gradients - a tutorial, the meter reader. Ed. B. VanNieuwenhuise, August issue, *The Leading Edge*, 941-949

Urrutia-Fucugauchi, J., Arellano-Catalán, O., Pérez-Cruz, L. *et al.* Chicxulub Crater Joint Gravity and Magnetic Anomaly Analysis: Structure, Asymmetries, Impact Trajectory and Target Structures 2022. *Pure Appl. Geophys.* **179**; https://doi.org/10.1007/s00024-022-03074-0

Vermeesch P., Morgan, J.V. 2008. Structural uplift beneath the Chicxulub impact structure. *J. Geophys Res* **113**: B07103; DOI: 10.1029/2007/JB005393

Vishnevsky, S., Montanari, A. 1999. Popigai impact structure (Arctic Siberia, Russia): Geology, petrology, geochemistry, and geochronology of glas-bearing impactites, in Dressler, B. O., Sharpton, V. L., Eds., *Large Meteorite Impacts and Planetary Evolution II:* Boulder, Colorado, The Geological Society of America, Special Paper 339

Whitehead J., Papanastassiou D. A., Spray J. G., Grieve R. A. F., Wasserburg G. J. 2000. Late Eocene impact ejecta: geochemical and isotopic connections with the Popigai impact structure. *Earth Planet. Sci. Letters* **181**, 473-487; https://doi.org/10.1016/S0012-821X(00)00225-9

Wichman, R. W. 1993. *Post-impact modification of craters and multi-ring basins on the Earth and Moon by volcanism and crustal failure*. Ph.D. thesis, Brown University (Providence, Rhode Island)

Zhang, F., Pizzi, A., Ruj, T., et al. 2023. Evidence for structural control of mare volcanism in lunar compressional tectonic settings. *Nat Commun* **14**, 2892; https://doi.org/10.1038/s41467-023-38615-1.